

# JGR Atmospheres

## RESEARCH ARTICLE

10.1029/2018JD028642

All authors contributed equally.

### Key Points:

- Significant interdecadal changes in temperature extremes are revealed, suggesting shortening of the winter season in Moscow
- Midwinter daily temperatures are less variable, but extant extremes are increasingly intense
- Moscow extremes are associated with North Atlantic and Mediterranean storm tracks and synoptic activity in the Barents-Kara Seas region

### Supporting Information:

- Supporting Information S1

### Correspondence to:

I. I. Zveryaev,  
igorz@sail.msk.ru

### Citation:

Zyulyaeva, Y. A., Studholme, J. H. P., & Zveryaev, I. I. (2019). Long-term changes in wintertime temperature extremes in Moscow and their relation to regional atmospheric dynamics. *Journal of Geophysical Research: Atmospheres*, 124, 92–109. <https://doi.org/10.1029/2018JD028642>

Received 8 MAR 2018



Accepted 14 DEC 2018

Accepted article online 17 DEC 2018

Published online 5 JAN 2019

©2018. American Geophysical Union.  
All Rights Reserved.

## Long-Term Changes in Wintertime Temperature Extremes in Moscow and Their Relation to Regional Atmospheric Dynamics

Yulia A. Zyulyaeva<sup>1</sup> , Joshua H. P. Studholme<sup>1</sup>, and Igor I. Zveryaev<sup>1,2</sup> 

<sup>1</sup>Shirshov Institute of Oceanology, Russian Academy of Sciences, Moscow, Russia, <sup>2</sup>Department of Meteorology and Climatology, Lomonosov Moscow State University, Moscow, Russia

**Abstract** Interannual variability and long-term changes in winter air temperature extremes in Moscow (1949–2017) are investigated using observational and reanalysis data. Significant interdecadal changes in principal characteristics of temperature extremes are revealed. Strong warming (0.50 °K per decade) is identified contrasting to the previously identified summer trend of 0.25 °K per decade. This is attributable to middle-to-late winter. Winter and summer daily air temperature variabilities are fundamentally different with wintertime anomalies strongly negatively skewed, while summer displays Gaussian variability. A reduction in the number of cold days and an increase in warm days in December and March are found. In January and February, the probability of warm extremes increases, while the probability of cold extremes remains constant. Intensification of January extremes (cold and warm) is revealed along with daily temperature variability reduction. In aggregate, potential shortening of Moscow's winter season, suppression of the previously strong seasonal cycle in daily temperature variability, and intensification of midwinter extremes are identified. Dynamical linkages are found to North Atlantic and Mediterranean storm track variability as well as synoptic activity over the Barents-Kara Seas. Lagrangian analysis shows associations of wintertime extreme warm events to air masses originating over the North Atlantic and Mediterranean regions. Air masses implicated in cold extremes are mostly of Siberian and Arctic origin. On interannual time scales cold event frequency in Moscow is impacted by the negative phase of North Atlantic Oscillation, whereas frequency of warm events is influenced by the positive phase of North Atlantic Oscillation and the negative phase of Scandinavian teleconnection.

**Plain Language Summary** A lot of contemporary research is currently focused on quantifying and understanding how global annual mean and seasonal mean warming impacts extreme events at the regional scale. Here we show that in Moscow changes to wintertime temperature characteristics suggest a potential shortening of the winter season. This is manifested in a warming of middle-to-late winter months, in an increasing number of extreme warm days in December and March and less day-to-day temperature changes in the middle of winter. Meanwhile, cold extremes are getting colder and warm extremes are getting warmer in the middle of winter. We show that cold extremes in Moscow are associated with air coming from Siberia and the Arctic regions. Warm extremes are formed by air advected from the North Atlantic and Mediterranean regions. We show that this is related to changes in the paths that weather systems originating in the North Atlantic take in getting to European Russia and thermal conditions over the Barents and Kara Seas.

### 1. Introduction

Extreme weather and climate events have drawn increased attention in recent years from both the theoretical and observational research branches of atmospheric science (e.g., Borodina et al., 2017; Coumou & Rahmstorf, 2012; Donat et al., 2016; Dosio & Fischer, 2018; Dwyer & O'Gorman, 2017; Pfahl et al., 2017; Sousa et al., 2018; Zhou & Khairoutdinov, 2017). This interest is justified in large part by extremes' disproportionate socioeconomic impact and due to projected increases in their frequency and intensity under climate warming scenarios (e.g., Christensen et al., 2007; Ballester et al., 2009; de Vries et al., 2012; Sura, 2014). Such extremes have particular relevance because they are local manifestations of large-scale, or even global, changes to the climate system (Bindoff et al., 2013). Temperature extremes are considered one of the most impact-relevant consequences of climate warming, but large uncertainties remain in our understanding principally at the local and regional scales (Intergovernmental Panel on Climate Change, 2012).

Europe is a densely populated region highly vulnerable to such extreme climate events, especially temperature extremes, both in winter and summer (Barriopedro et al., 2011; Beniston, 2004; Schär et al., 2004; Sillmann et al., 2011; Sousa et al., 2018; Tebaldi et al., 2006). As Europe's most populated city, with a population over 12 million (United Nations, Department of Economic and Social Affairs, Population Division, 2015), Moscow is a particular area of interest. Furthermore, Moscow is one of the highest latitude and coldest metropolises on Earth, making it even more vulnerable to extreme climate events. Wintertime extremes at such high latitudes can shift temperatures across the freezing point of water, which amplifies their impact. Therefore, an improved understanding of the characteristics and physical mechanisms of regional temperature extremes (both cold and warm) could enhance our capacity for predicting regional climate anomalies. This in turn will allow for knowledge-based adaptation and mitigation strategies.

As the most prominent climate signal in the North Atlantic-European region, the North Atlantic Oscillation (NAO) is known to be significantly associated with European climate on a range of time scales (e.g., Hurrell, 1995). This relationship is particularly strong during boreal winter when the NAO is most pronounced (e.g., Zverevaev, 2006; Zverevaev & Gulev, 2009). Studies suggest linkages between wintertime climate extremes in Europe and the NAO (e.g., Cattiaux et al., 2010; Luo, 2005). Specifically, it has been shown that during its negative phase (i.e., a state of weakened meridional pressure gradient), the NAO contributes significantly to extreme cold events in Europe such as was observed in the winter of 2010 (e.g., Cattiaux et al., 2010; Wang et al., 2010). Diao et al. (2015) revealed an asymmetry in European winter temperature extremes and their relation to the NAO. This is reflected in the larger magnitudes of cold extremes as well as in different locations of the major action centers of temperature extremes. Furthermore, Chen and Luo (2017) showed that strong cold anomalies over northern Europe are associated with quasi-stationary Greenland blocking, which in turn is related to the negative phase of the NAO. This may be triggered by Arctic sea ice reduction (e.g., Screen, 2017a).

Zhong et al. (2018) highlight the important role of atmospheric moisture advection in sea ice reduction and regional warming in Barents-Kara Seas (BKS) basin. They demonstrate that meridional moisture transport is the major player in recent BKS warming. They further show that enhanced moisture transport into BKS region is associated with a pattern similar to that of the positive phase of the NAO and more easterly located Ural blocking. Since warming in BKS region is associated with cold anomalies over continents (e.g., Overland et al., 2011; Shepherd, 2016), this result is somewhat contradictory to previous studies showing that wintertime low temperatures in Europe are associated with the negative phase of the NAO as it was particularly observed in winter 2009/2010 (e.g., Overland et al., 2011). Moreover, Cohen et al. (2012) demonstrate that regional Northern Hemisphere wintertime cooling is directly tied to the downward trend in the wintertime Arctic Oscillation (which is structurally similar to the NAO).

Although the NAO impacts to varying degrees the entire European region, it should be noted that, due to its location in the most eastern part of Europe, Moscow's climate and its extremes may potentially be less impacted by the NAO. Thus, other additional factors may play important roles. This leaves a significant gap in our understanding. Another potentially relevant climate phenomenon is the so-called Arctic amplification (Cohen et al., 2014; Francis & Vavrus, 2012; Serreze & Francis, 2006) associated with the Arctic sea ice reduction (e.g., Chen & Luo, 2017; Screen, 2017a, 2017b) and with the warm Arctic-cold continents pattern (e.g., Overland et al., 2011). Arctic amplification implies faster rates of warming at high latitudes in comparison to lower latitudes. This results in a reduced meridional temperature gradient between the Arctic and lower latitudes and changes geopotential height structure and seasonal climate variability. Consequently, this potentially results in decreased intraseasonal temperature variability in northern and midlatitudes during the cold season by amplification of planetary waves and more persistent weather patterns (e.g., Screen, 2014; Screen & Simmonds, 2014). Again, it should be noted that Moscow is somewhat outside the major cooling center over Eurasia normally associated with the warm Arctic-cold continents pattern (see, e.g., Figure 2 in Shepherd, 2016). For an excellent review of the complex, numerous and nonlinear potential mechanisms associated with Arctic amplification and midlatitude extreme events the interested reader is directed to Overland et al. (2016).

It can be expected that besides Arctic amplification and the NAO, other regional atmospheric teleconnections (e.g., Scandinavian and East Atlantic-Western Russia teleconnections, Barnston &

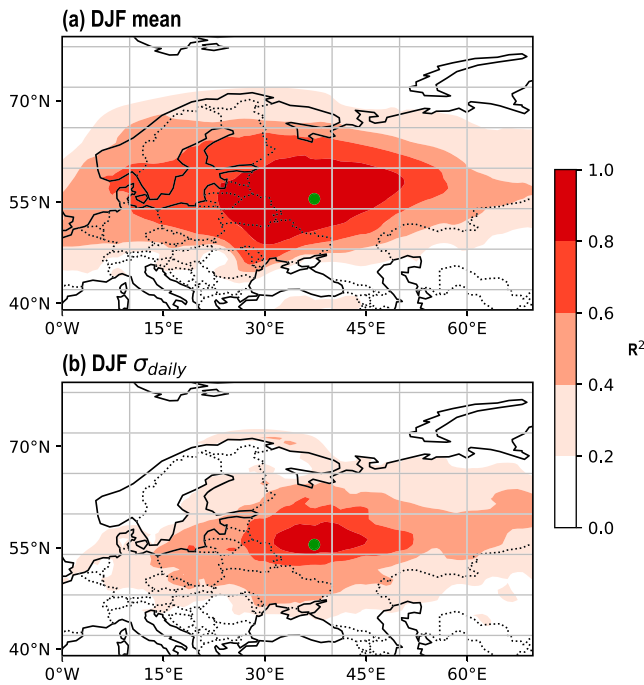


**Figure 1.** Coefficient of determination,  $R^2$ , between the VDNH station and ERA-Interim 2-m temperature for the DJF seasonal mean (a) and the standard deviation of DJF daily temperatures (b). DJF = December-January-February.

Livezey, 1987) may play roles. Luo, Xiao, Diao, et al. (2016) and Luo, Xiao, Yao, et al. (2016) suggest that wintertime Eurasian cold anomalies are impacted, in addition to the NAO, by Ural blocking, which is associated with sea ice reduction in the Barents Sea and the positive phase of the NAO. This makes elucidating and understanding the mechanisms driving temperature extremes rather complex. Hence, further analysis of regional temperature extremes and associated processes is necessary.

This study explores wintertime cold and warm air temperature (AT) extremes in Moscow and the long-term time evolution of their principal characteristics (intensity, frequency of occurrence, and duration) during recent decades. We investigate linkages to atmospheric dynamics in the North Atlantic-European sector over a range of time scales and analyze the origin of air masses implicated in the formation of AT extremes. The data used and the analysis methods are described in section 2. The time evolution of the statistical characteristics of wintertime AT extremes is considered in section 3. In section 4 we examine the relationships of these extremes to regional-scale atmospheric dynamics and, based on Lagrangian back trajectories, analyze the origin of air masses associated with these extreme events. Finally, a summary and a short discussion are provided in section 5.

## 2. Data and Methods

### 2.1. Observational and Reanalysis Data

We employ observational daily AT data at the 2-m level from the data set described by Razuvaev et al. (1993). This data set includes observations from 223 meteorological stations around the former Soviet Union. We use data for

Moscow VDNH (World Meteorological Organization, WMO code 27612) as this station provides one of the longest unbroken time series for the region of interest (i.e., European Russia). A total of 69 winters (December-January-February, DJF) for the period 1949–2017 is analyzed. Over this period, period-mean DJF-mean temperature in Moscow was  $-6.93$  °C with a standard deviation,  $\sigma$ , of 2.4 °C. Typical wintertime daily temperature variability, as measured by period-mean DJF-sigma in daily temperature means, was 6.22 °C. Detailed information on the data processing and the data set construction can be found in Razuvaev et al. (1993).

For the Lagrangian analysis of back trajectories we employ three-dimensional 6-hourly ERA-Interim reanalysis data (Dee et al., 2011) on a regular  $3/4^\circ$  latitude-longitude grid. The ERA-Interim period is 1979 to present; trajectories analyzed in the present study therefore are for events covering the period 1979–2017. To analyze links to regional synoptic-scale dynamics, we use daily geopotential heights at the 850-hPa level,  $Z_{850\text{hPa}}$ , also from ERA-Interim. We use this level since it is low enough to capture shallow, fast moving extratropical cyclones but also minimizes any potential influence of topography.

We use indices of the major teleconnection patterns that have been documented and described by Barnston and Livezey (1987). The patterns and indices were obtained by applying rotated principal component analysis (e.g., Hannachi et al., 2007) to standardized 500-hPa height anomalies in the Northern Hemisphere. The teleconnection patterns used here to examine links to AT extremes include the NAO, East Atlantic (EA), East Atlantic-West Russia, and the Scandinavian (SCAND) patterns. They are regularly updated indices, covering the period 1950 to present, and are available from the National Oceanic and Atmospheric Administration Climate Prediction Centre website. Further details on the teleconnection pattern calculation procedures can be found in Barnston and Livezey (1987) and at the Climate Prediction Centre website. These indices have been curtailed to match the period of analysis.

While Moscow temperature extremes are themselves worth studying, we show that temperature variability there is well correlated with a broader region (Figure 1). Seasonal mean 2-m AT from the VDNH station data shares  $>80\%$  of its variability with corresponding temperature in ERA-Interim over European Russia, the Baltic States, Belarus, and northeast Ukraine (Figure 1a). By contrast, cooccurrence of temperature extremes, as proxied by the standard deviation,  $\sigma$ , of daily temperature is much more local (Figure 1b). The  $>80\%$  contour is constrained to a region of approximately 1,000 km<sup>2</sup> centered just north of Moscow.

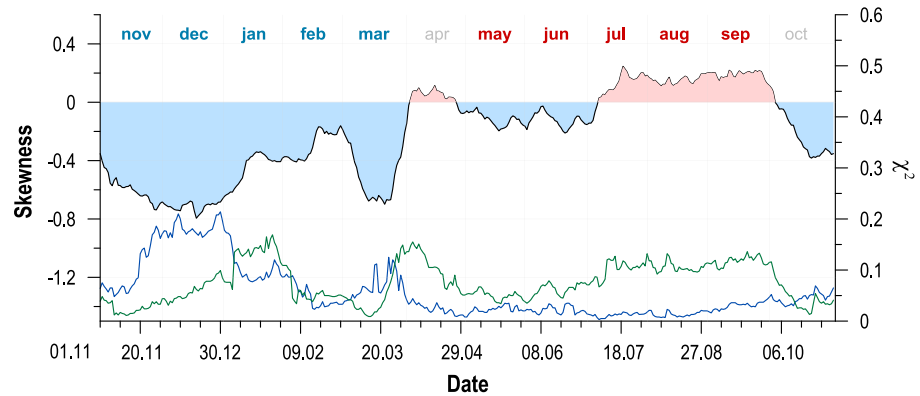


**Figure 2.** Coefficient of skewness (black curve) of the empirical distribution of winter daily air temperature (calculated over the reference period 13 October 1960 to 19 December 1990) for the VDNH station, Moscow. Pearson's criteria for Gaussian distribution (blue line) and for the asymmetric distribution (green line) are defined in equation (1).

## 2.2. Extreme Event Identification

We define wintertime AT extremes using a four-step approach described in detail in Zyulyaeva et al. (2016) where summertime temperature extremes were analyzed. This is a percentile-based approach commonly used to analyze extremes (e.g., Alexander et al., 2006; Diao et al., 2015). We use the base period 1961–1990 (i.e., the standard WMO reference period; World Meteorological Organisation, 2015). This period and percentile-based approach are also recommended by the Climate Variability and Predictability Expert Team on Climate Change Detection, Monitoring and Indices (Klein Tank et al., 2009). To remove inhomogeneities and thus eliminate possible bias in trend estimation, we applied the “jump” removing algorithm of Zhang et al. (2005).

We remove the seasonal cycle as approximated by a fourth-order polynomial (estimated for 1961–1990) from daily AT (see Figure 1 in Zyulyaeva et al., 2016). We then construct empirical occurrence histograms (EOH or observed frequency distributions) for each day of the winter season for the reference period (1961–1990). We use data from 25 consecutive days centered upon the day of interest (further referred to as 25CD). Thus, to construct EOHs for each day we have a  $25(\text{days}) \times 30(\text{years}) = 750$  sample size. We then fit EOHs with an analytical probability density function (PDF) to improve the stability of distribution statistics derived from the data (e.g., Folland et al., 1999; Coles et al., 2001). Since our analysis reveals a fundamental asymmetry in the AT EOHs during the cold season, as analytical representations of EOHs we consider not only the normal (i.e., Gaussian) distribution but additionally an asymmetric (skewed) distribution whose PDF,  $P(x)$ , is given by

$$P(x) = \alpha\beta \exp(-\beta x) \exp[-\alpha \exp(-\beta x)], \quad (1)$$

where  $\alpha$  and  $\beta$  are steering parameters computed in fitting  $P(x)$  (e.g., Gulev & Belyaev, 2012). For each day we estimate the Pearson criteria (i.e.,  $\chi^2$ ) for both these analytical distributions (Figure 2). This allows us to determine which distribution optimally represents that each day's temperature variability. Figure 2 shows that over the extended winter season (October–March) skewness is essentially negative and large (reaching  $-0.8$  in December) implying that the asymmetric distribution fits better to the observed frequency distribution. This is particularly true for December. Note that during the warm season, skewness is small and mainly positive suggesting that a Gaussian distribution fits better to the observed frequency distribution in this season (Figure 2). Consequently, we characterize each day by the distribution with the lowest  $\chi^2$ .

Finally, using a cumulative distribution function,  $C(x)$ , based on the sample expected value and  $\sigma$ , we convert AT anomalies into percentiles. The Gaussian  $C(x)$  is a standard reference (e.g., Zwilling, 2002), while the  $C(x)$  corresponding to  $P(x)$  in equation (1) is derived here as

$$C(x) = \exp[-\alpha \exp(-\beta x)] + \text{const.} \quad (2)$$

To investigate the characteristics of wintertime cold and warm events, we define a particular extreme event as a period when the daily AT anomalies exceed an established threshold (10th percentile for cold events and 90th percentile for warm events) for at least three consecutive days.

### 2.3. Trajectory Computation and Classification

To identify the origin of air masses implicated in extreme events, we compute their 5-day Lagrangian back trajectories. Trajectories are computed for all warm [ $P(90\text{th})$ ] and cold [ $P(10\text{th})$ ] events with the Lagrangian analysis solver (LAGRANTO; Sprenger & Wernli, 2015) using the ERA-Interim reanalysis three-dimensional wind field at 60 model levels. Lagrangian analysis solves the trajectory equation  $D\mathbf{x}/Dt = \mathbf{u}(\mathbf{x})$ , where  $\mathbf{x} = (\lambda, \varphi, p)$  is the position vector in natural coordinates and  $\mathbf{u} = (u, v, \omega)$  is the three-dimensional wind vector. The interpolation specifics and implementation details can be found in Sprenger and Wernli (2015).

Back trajectories were initialized from 37.37°E, 55.45°N and computed at every level between 1,000 and 850 hPa at 5 hPa intervals. At lower levels, trajectory initiation is sometimes attempted at higher pressures than the realized surface pressure (i.e., a trajectory from 1,000 hPa may not be computed if the surface pressure is 985 hPa). In such cases, no trajectory may be computed. To avoid this issue, we note that for present purposes there is negligible difference for trajectories started between 1,000 and 850 hPa and as such only parcels located at 900 hPa at  $t = 0$  hr are shown here. All conclusions discussed are identical as for lower levels. There is small vertical motion relative to horizontal motion over considered time scales and as such, only the horizontal component of trajectories is shown.

We classify trajectories based on their 5-day origin (between times  $-96$  and  $-120$  hr). The choice of 5 days is supported by scale analysis of synoptic motions, which suggests we are interested in processes occurring over  $O(1)$  days (e.g., Holton & Hakin, 2013) as well as the typical definition of blocking (5 days, e.g., Woollings et al., 2018). Similar timeframes have been used in Lagrangian analysis of similar processes (e.g., Fuchs et al., 2017; Papritz & Spengler, 2017; Schemm et al., 2016; Schemm & Schneider, 2018).

We use a formal unsupervised classification methodology, specifically  $K$ -means clustering (e.g., Lloyd, 1982). We chose the number of classes for both cold and warm events based separate qualitative sensitivity tests. Since we are presently interested in discussing the origin of air masses, we choose the number for each extreme event type that corresponds to reasonable and intuitive descriptions of said origins. For example, fast moving versus slow-moving cyclones and western European versus Arctic origin. Ultimately, the number of types chosen is a subjective imposition onto the data, but the limitations of this are not grave in this context. The classification is useful for discussing different types of event and indicating further more physically based analysis. Given a chosen number of classes, the clustering is repeated 10,000 separate times and the classification with the highest inertia is chosen. The scikit-learn implementation of this algorithm is used (Pedregosa et al., 2011).

## 3. Major Characteristics of Winter Temperatures in Moscow and Their Long-Term Evolution

### 3.1. Changes in Daily Temperature PDFs

European Russia is characterized by large AT variability at different time scales. In particular, the amplitude of the AT annual cycle is the largest of all Europe, exceeding 17 °C (e.g., Zveryaev, 2007). Additionally, it should be emphasized that the magnitude of wintertime European AT interannual variability is maximal over European Russia and southern Scandinavia (see, e.g., Figures 1a and 3a in Zveryaev & Gulev, 2009). AT variability at shorter (e.g., synoptic) time scales is also large in this region and often associated with blocking events (Sousa et al., 2018; Tyrlis & Hoskins, 2008). Therefore, from a climatological perspective large wintertime temperature fluctuation in Moscow and in European Russia in general are not unusual.

To investigate the principal characteristics of wintertime AT daily anomaly PDFs and their changes over recent decades, we analyze the variability of the PDF mean,  $\sigma$ , and skewness. PDFs have been constructed for each winter day throughout the extended winter season (October–April) with a 21-year running window with 1-year time step. The 25CD type of subsampling has been applied. A positive trend in mean AT is well pronounced during middle-to-late winter (Figure 3a). This is generally consistent with an earlier detected intensification of global warming starting in the 1970s (e.g., Intergovernmental Panel on Climate Change, 2014). However, this warming trend is notably absent from the early winter season (i.e., November–December). In December, there is no significant trend in mean temperature anomalies or  $\sigma$ , but we do see

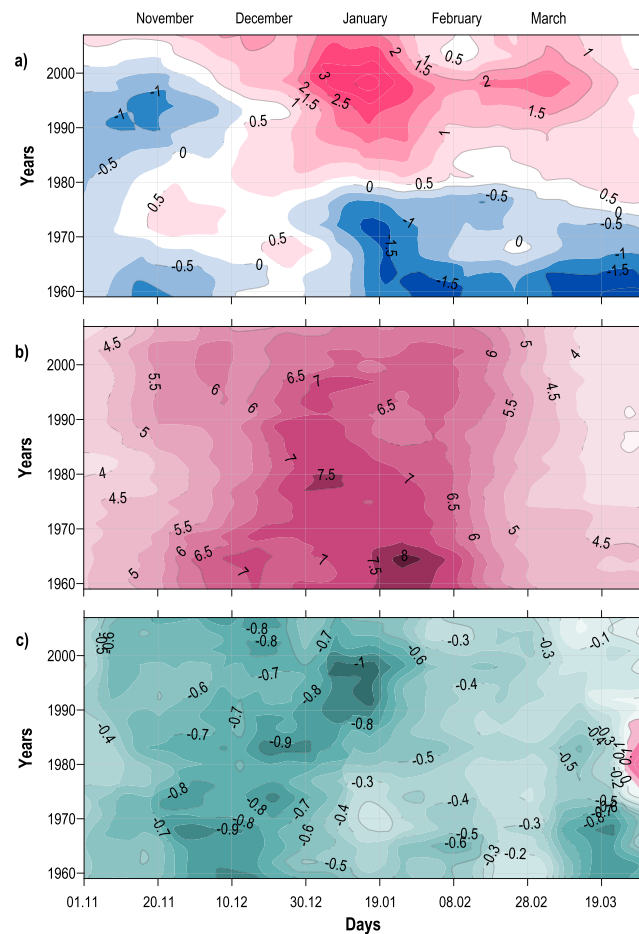


**Figure 3.** Time evolution of probability density function (a) mean, (b)  $\sigma$ , and (c) skewness for the wintertime daily air temperature anomalies.

notable changes in the PDF skewness (Figure 3c). Over the entire period it has become increasingly symmetric implying that in comparison to the 1960s (when during December cold events were more probable), in the most recent decade the probabilities of positive and negative anomalies in December have been more or less equal.

The most remarkable changes occur in January when a negative trend in  $\sigma$  shows a squeezing of the PDF toward the mean values (Figure 3b). In fact, this implies that January temperatures have become on average less variable; that is, the probability of low, or even 0, magnitude temperature anomalies has increased. Coincident with this decline in overall daily temperature variability, strongly increasing negative skewness shows growing PDF negative asymmetry (Figure 3c). This implies an increasing probability of observed moderate temperature anomalies during the last 30 years being cold. However, relative to the base period, increasingly negative skewness and this associated redistribution of probability density toward the right tail implies more temperatures exceeding the warm extreme threshold than the cold extreme threshold (Figure 4b, area between solid and dashed red lines). On top of this, the absolute magnitude of cold temperature anomalies has also increased from 17.5 to 22.5 °C (Figures 4a and 4b). So over all, the changes in the middle of winter are quite nuanced and require careful consideration but represent fundamental changes to wintertime climate.

In March, that is, the final winter month, as in January and February there is a warming trend albeit of a slightly lower magnitude to that of the midwinter (Figure 3a). However, in stark contrast to January, March's PDF skewness is initially strongly negative but has very much declined over the entire period

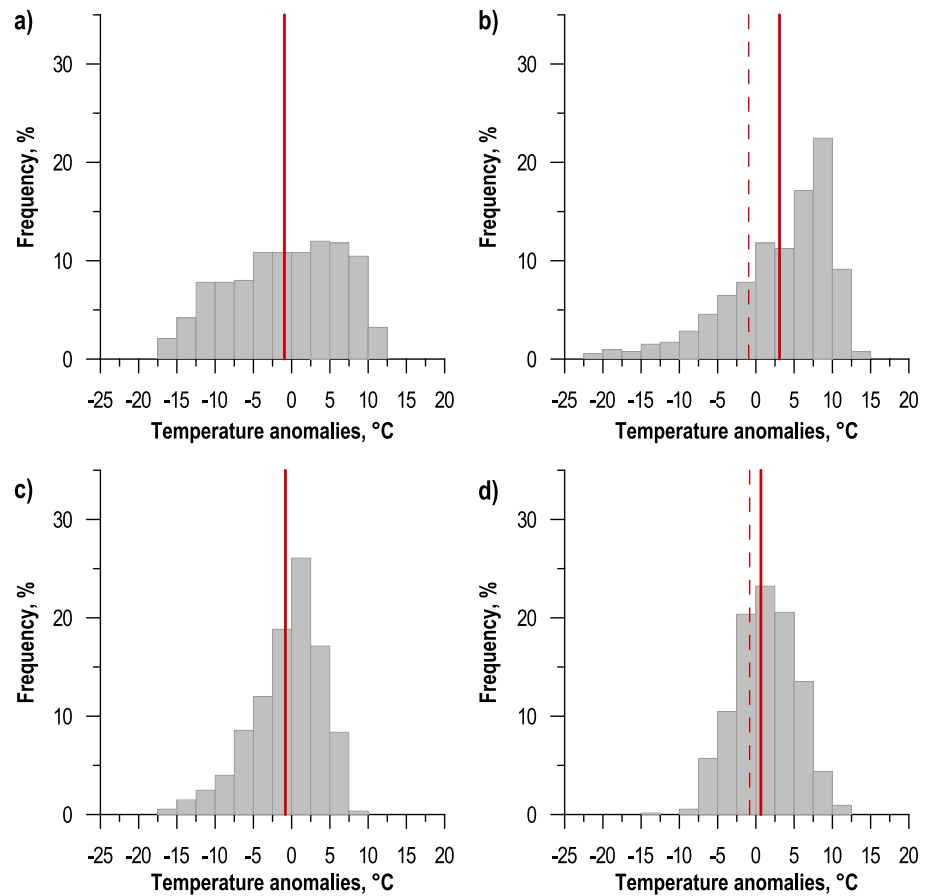


**Figure 4.** Empirical occurrence histograms of daily temperature anomalies for January (a, b) and March (c, d) for period 1958–1978 (a, c) and 1987–2007 (b, d). Subsampling means are marked by solid red lines, and means of the 1958–1978 period are marked as dashed red lines in (b) and (d). These two 21-years periods are chosen since they most clearly demonstrate characteristic changes (see Figure 3).

(Figure 4c). Again, January’s skewness in the earlier decades is fairly negligible but has become more negative in recent decades (Figures 4a and 4b). This implies that the occurrence probability of warm temperature anomalies in this final winter month has increased (i.e., the opposite of what we find in January, Figure 4).

Results indicate a very strong seasonal cycle in daily temperature variability (Figure 3b). Early (i.e., November) and late (i.e., March) winter temperatures are characterized by smaller  $\sigma$  in comparison to mid-winter months. Looking over the entire period, we see an increasing suppression in this seasonal cycle, characterized by a reduction in January and February daily temperature variability. This appears to be consistent with the findings of Screen (2014).

Therefore, these results demonstrate that the regional manifestation of global warming during recent decades is associated, not only with an increase of the seasonal mean AT (which is reflected in the increase of PDF means during middle-to-late winter months) but also with changes in the shape of these PDFs. Summarizing these trends, results suggest the following:

1. A warming of middle-to-late winter months, that is, January through March, but not early winter.
2. A suppression of the strong seasonal cycle in daily temperature variability driven by a reduction in January and February variability.
3. A tendency for temperature anomalies in January to be lower magnitude in recent decades but strong fluctuations from this mean are increasingly likely to be cold rather than warm. At the same time cold extremes are increasingly intense.

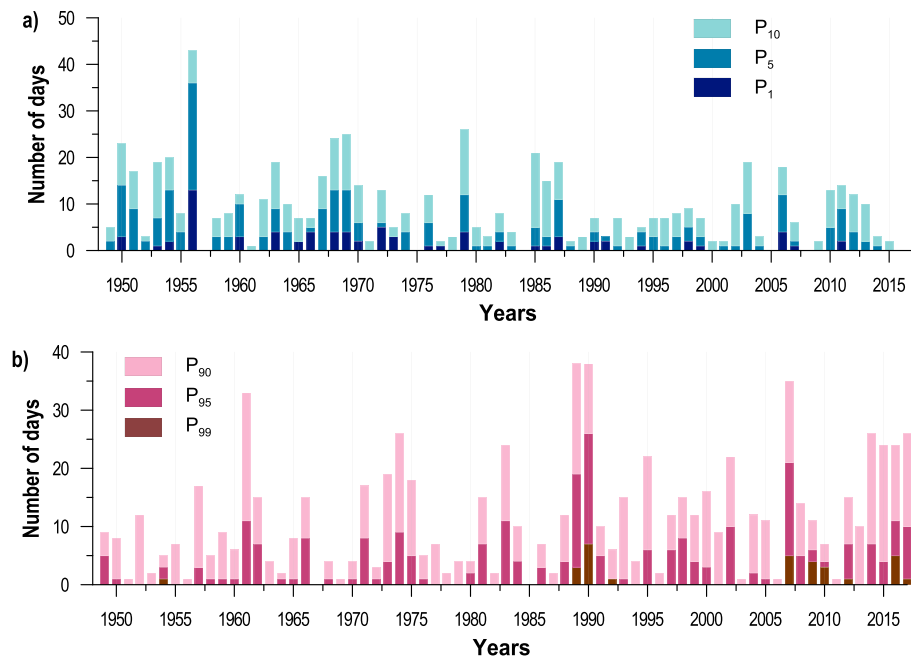


**Figure 5.** Total number of days (December-January-February) with (a) negative and (b) positive air temperature anomalies meeting thresholds: 1st, 5th, and 10th percentiles for a cold days (a) and 90th, 95th, and 99th percentiles for a warm days (b).

4. Additionally, due to strong warming of mean January temperatures relative to early decades the probability of warm extremes as defined relative to earlier climates (e.g., the 1960s) has increased.
5. An increasing probability of warm extremes during March and December.

### 3.2. Changes in Extreme Temperature Event Frequency and Duration

We next analyze the number of days in each winter season for which daily AT anomalies exceeded certain thresholds. The total number of anomalously cold and warm days is shown respectively in Figures 5a and 5b. We define thresholds of the 10th, 5th, and 1st percentiles for the negative AT anomalies (Figure 5a) and 90th, 95th, and 99th percentiles for the positive AT anomalies (Figure 5b). In terms of long-term trend-like changes we find a general tendency toward a decrease in the number of extremely cold days in Moscow (Figure 5a) and a corresponding increase in the number of extremely warm days (Figure 5b). This trend is not necessarily representative of specific interdecadal variability however, and over last 25 years there is a trend toward an increased number of extremely cold days (this is also seen in Figure 10).

We now turn to EOHs for the duration of cold and warm extreme events with daily AT anomalies exceeding, respectively, thresholds 10th and 90th percentiles (Figure 6). For the period analyzed there are 142 cold events within the 10th percentile threshold. The duration of cold events varies from 3 to 17 days (Figure 6). The shortest (i.e., 3 days) events are most frequent (representing about 40% of the total number of cold events), while events lasting longer than 7 days are relatively rare (less than 5% of total number). There are 159 warm events within the 90th percentile threshold. Their length varies from 3 to 23 days (Figure 6). In general, we observe an exponential distribution for the duration of extreme events, both warm and cold. The *e*-folding of the cold event EOH is somewhat shorter than for the warm events (Figures 6). This implies a larger role of short-term (3–5 days) events in cold events.

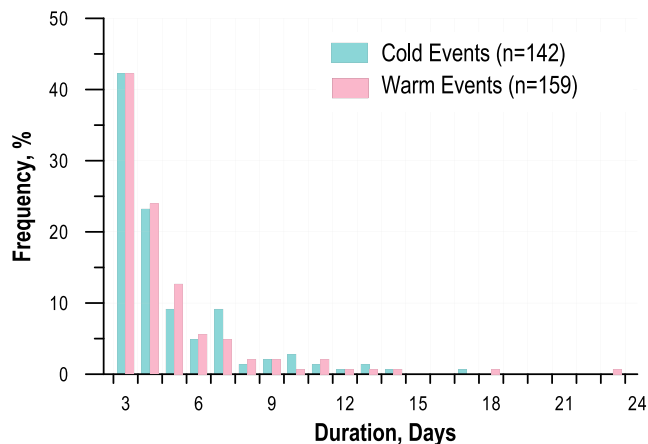


**Figure 6.** Empirical occurrence histograms of duration of the extreme events with air temperature anomalies exceeding thresholds 10th (blue) and 90th (pink) percentiles.



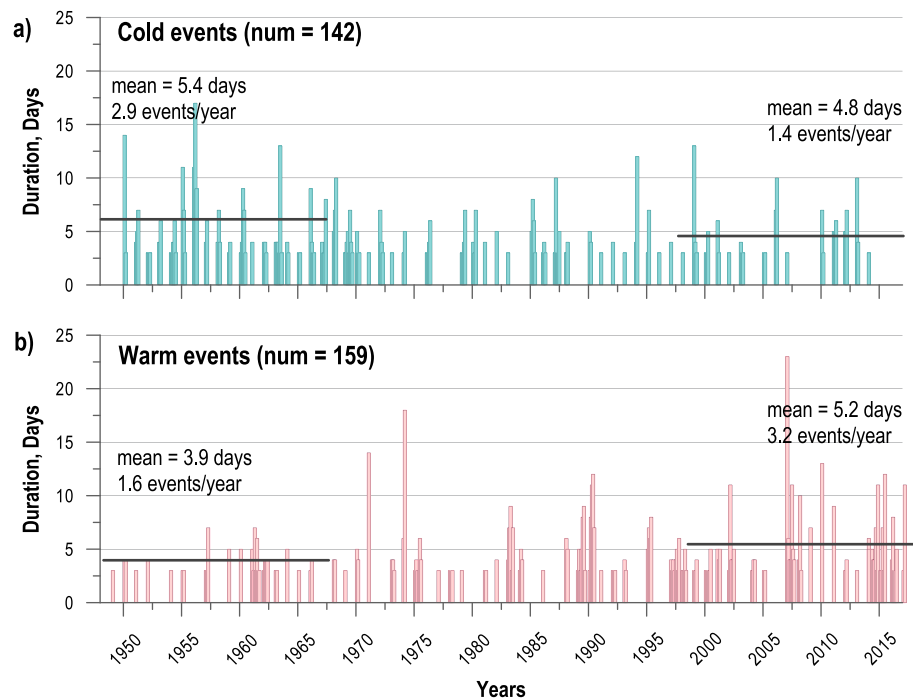


**Figure 7.** Duration of the cold (a) and warm (b) events with air temperature anomalies exceeding thresholds 10th and 90th percentiles, respectively. Mean event durations and the frequency of the events for the first and last 20 years are shown in bold black lines; these years are significantly different for warm events (duration and frequency) and for the frequency of the cold events at the 5% level according to Student's  $t$  test. They are not significantly different for the duration of the cold events.

Finally, Figure 7 shows all detected cold (10th percentile) and warm (90th percentile) events and their duration. A noticeable increase in the duration and frequency of warm events during most recent decades is also evident. In the last 20 years the frequency of the warm events has doubled (Figure 7b). At the same time the frequency of the cold events dropped from 2.9 events per year to 1.4 events per year. This is generally consistent with results of our analysis of EOHs (Figure 6).

## 4. Links to Atmospheric Dynamics in the North Atlantic-European Sector

### 4.1. Air Mass Origins

To define the major air masses involved in formation of the wintertime cold and warm extreme events, we compute the Lagrangian back trajectories for air parcels at 900 hPa and classify them as described in section 2. As seen from Figure 8a, the majority of trajectories associated with cold events in Moscow indicate that air masses implicated in these extreme events do indeed come from the north and northeast (i.e., from climatologically colder regions), whereas trajectories associated with warm events clearly indicate that air masses forming these events arrive mostly from the west and southwest.

We further objectively classify cold events into three types. Type 1 events (27% of all cold events) are of oceanic origin indicating that the majority of relevant trajectories originate in the northeastern North Atlantic-Arctic sector from Scandinavia to Greenland (Figure 8b). Type 2 events (11.1% of all cold events) are of polar origin with trajectories originating mostly in the central Arctic basin. Finally, more than half (61.9%) of all cold events are type 3 events characterized by prevailing relatively slow advection of cold air from the east and northeast (Figure 8b).

Warm events are mostly comprised of type 1, type 2, and type 4 events, which account for a fairly comparable proportion each (Figure 8c, 32.7%, 34.6%, and 26.2%, respectively). The major source regions for these air masses are western Europe (type 1 associated with the slow-moving cyclones), the Mediterranean (type 2) region, and the western North Atlantic (type 4 associated with the fast-moving cyclones; Figure 8c). Warm events of type 3 play a very minor role (6.5% of all warm events) and demonstrate links to air

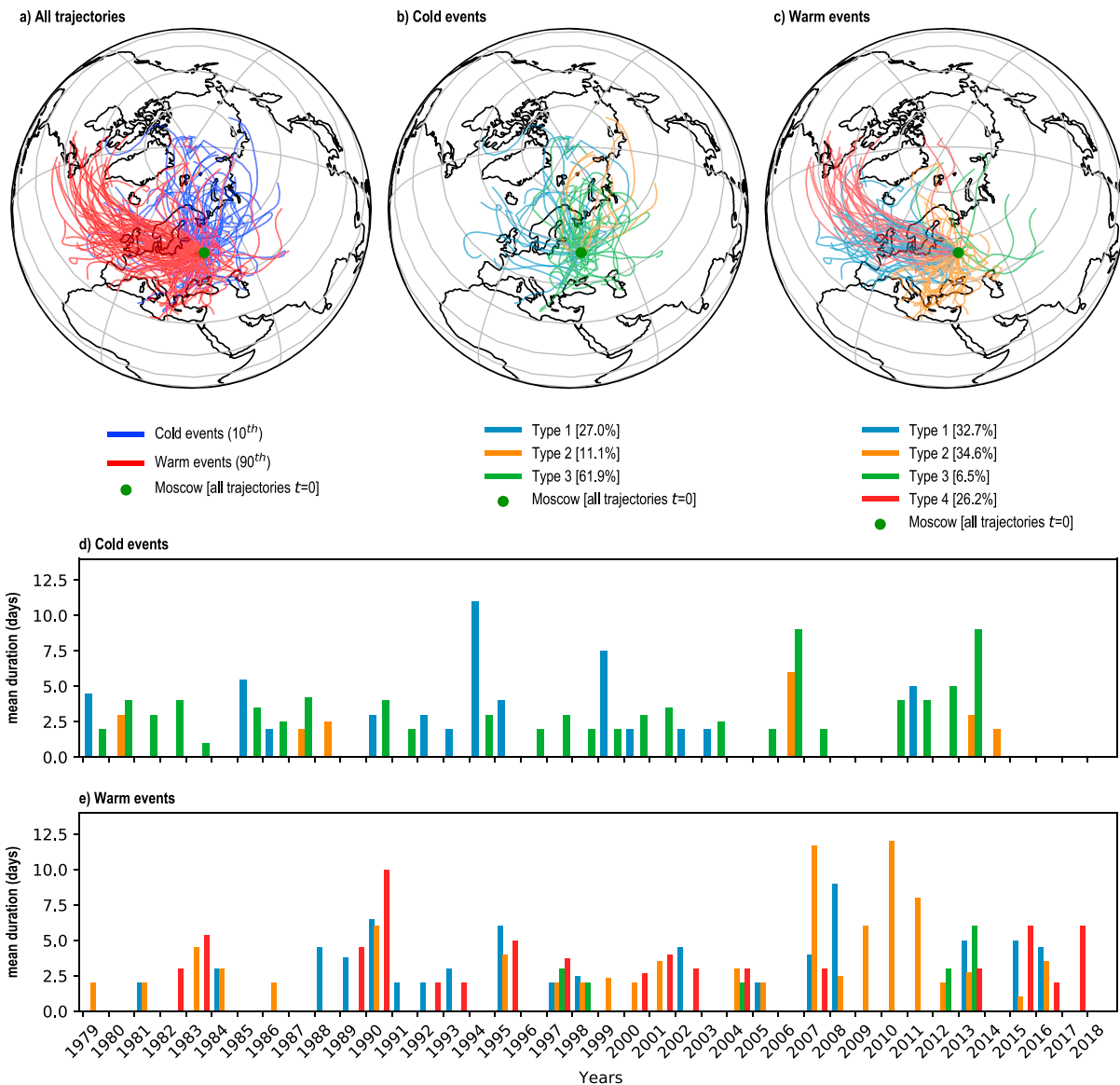


**Figure 8.** Lagrangian back trajectories of air masses at 900 hPa implicated in Moscow cold and warm extreme events. (a) All trajectories divided by associated Moscow temperature extreme. Trajectories classified by origin for cold and warm extremes are plotted separately in (b) and (c), respectively. The length of the (d) extreme cold (10th percentile) and of the (e) extreme warm (90th percentile) events; the colors match the type of the trajectories.

masses of eastern origin. This is a somewhat controversial result that can be explained either by local diabatic heating in the vicinity of Moscow or by some deficiencies in the analysis method.

During recent decades cold events became less frequent (Figure 8d). At the same time, warm events were more frequent and their duration increased (Figure 8e). This is consistent with Figure 7. For the cold extremes (Figure 8d) during the last 15 years we find only one winter when the type 1 trajectory has been detected. On the other hand, in 1990–2003 there were eight winters with the type 1 trajectories detected. It is also seen that events with type 3 trajectories, corresponding to advection from the BKS region tended to last longer (increased duration). This result is in direct agreement with results of Shukurov and Semenov (2018). For warm extremes (Figure 8e) there was an intensification of the warm air advection from the Mediterranean Sea region (type 2 trajectories) during the last 15 years, whereas advection from the western Europe (type 1 trajectories) decreased. The limited number of type 4 trajectories in 2005–2015 can be explained by the predominantly negative phase of the NAO and associated weakening of the westerly flow over the considered time period.

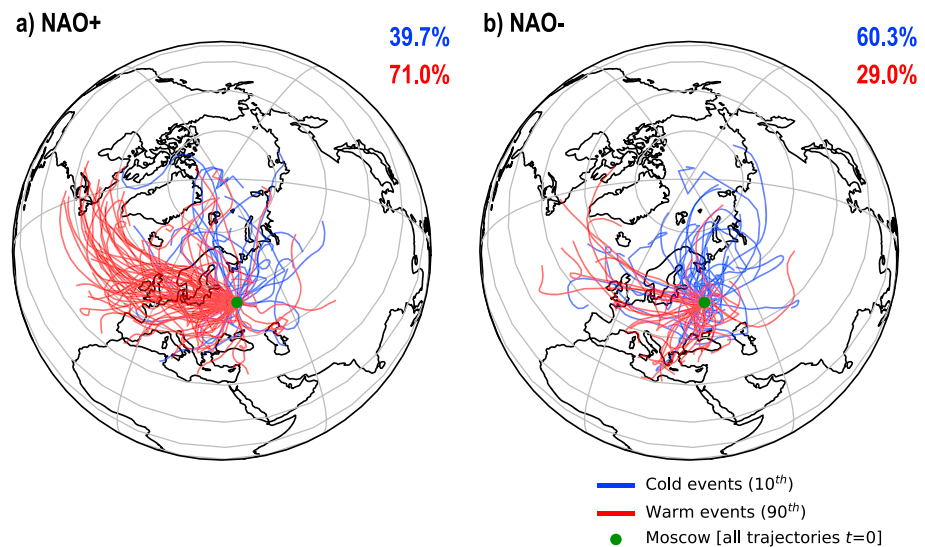


**Figure 9.** As for Figure 8 but with trajectories divided based on positive (a) and negative (b) phases of the NAO. Blue (red) colors indicate cold (warm) events and percentages correspond to the total fraction of the event type during the respective NAO phase. NAO = North Atlantic Oscillation.

#### 4.2. Links to Regional Atmospheric Teleconnections

We further examine links between wintertime AT extremes in Moscow and major regional teleconnections. To do this, we estimate correlations between time series of the number of cold and warm days in Moscow during each winter (DJF) and indices of the NAO, SCAND, East Atlantic-West Russia, and EA teleconnections (Barnston & Livezey, 1987) for winters 1948/1949–2016/2017. Here we only discuss correlations that are statistically significant at the 5% level according to the Student's  $t$  test (Bendat & Piersol, 1966). All computed correlations are provided in the supporting information as Table S1. Clearly, the NAO most significantly impacts interannual variability of the number of cold days. Specifically, a negative correlation between respective time series ( $-0.48$ ) indicates that cold extremes in Moscow occur during the negative phase of the NAO characterized by the weakening of the North Atlantic storm track and reduced advection of warm air into the European region.

Warm extremes in Moscow are associated with the NAO and the SCAND teleconnections (see Table S1). Positive ( $0.61$ ) correlation to the NAO index and negative ( $-0.35$ ) correlation to the SCAND index suggest that the warm events occur during positive phase of the NAO (NAO+) resulting in enhanced warm air advection from the North Atlantic region. Likewise, during the negative phase of the SCAND (SCAND-) such advection is enhanced in the Mediterranean region. Note that this result is in excellent agreement with above back trajectories analysis, which reveals comparable roles of these sources of warm, moist air in the formation of wintertime warm extremes. We also find significant correlation between the EA teleconnection and warm days ( $0.31$ ). In some studies (e.g., Moore et al., 2013) the EA is considered as a zonally shifted (toward the east) form of the NAO. Thus, our results imply that the EA exerts a similar but essentially weaker impact on the cold and warm temperature extremes in Moscow as the NAO. Having stated this, we limit our further analysis to the links between temperature extremes in Moscow and the NAO and SCAND teleconnections.

To get further insight into relationships between extreme events in Moscow and different phases of the NAO and SCAND, we show trajectories corresponding to positive and negative phases of these teleconnections (Figure 9 for NAO and supporting information Figure S1 for SCAND). The number of trajectories associated with cold extremes is essentially larger during the negative phase of the NAO (NAO-,  $60.3\%$ ) than that during NAO+ ( $39.7\%$ ; Figure 9). Consistent with the above analysis, during NAO- trajectories associated with cold extremes are mostly of Arctic-northern Siberian origin (Figure 9b), which is evidently not the case for NAO+ (Figure 9a). During NAO+ (i.e., an increased meridional pressure gradient), the number of trajectories ( $71.0\%$ ) associated with warm extremes is more than double than that during NAO- ( $29.0\%$ ,

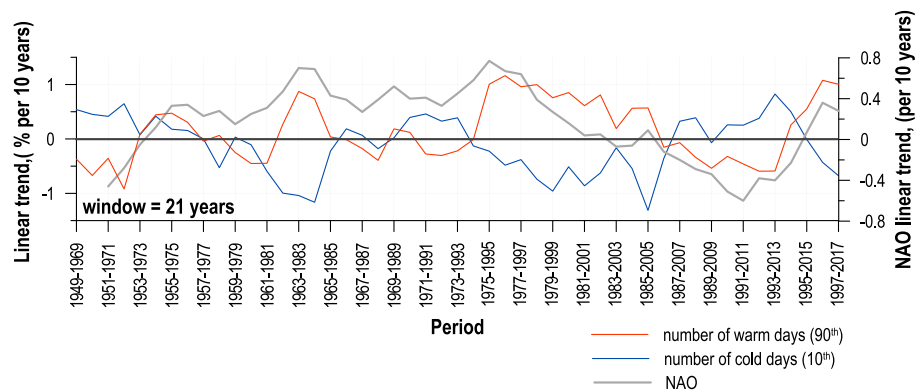


**Figure 10.** Time series of linear trends of the number of extremely warm (90th percentile; red curve) and cold (10th percentile; blue curve) days estimated for the 21-year running window with a 1-year lag. Red and blue lines indicate long-term changes of trends estimated respectively for the days with positive and negative air temperature anomalies. NAO = North Atlantic Oscillation.

Figures 9a and 9b). Principal difference in the respective trajectories patterns is also evident between the two NAO phases with trajectories originating predominantly in western North Atlantic during NAO+ and trajectories of somewhat different origins during NAO– (Figures 9a and 9b).

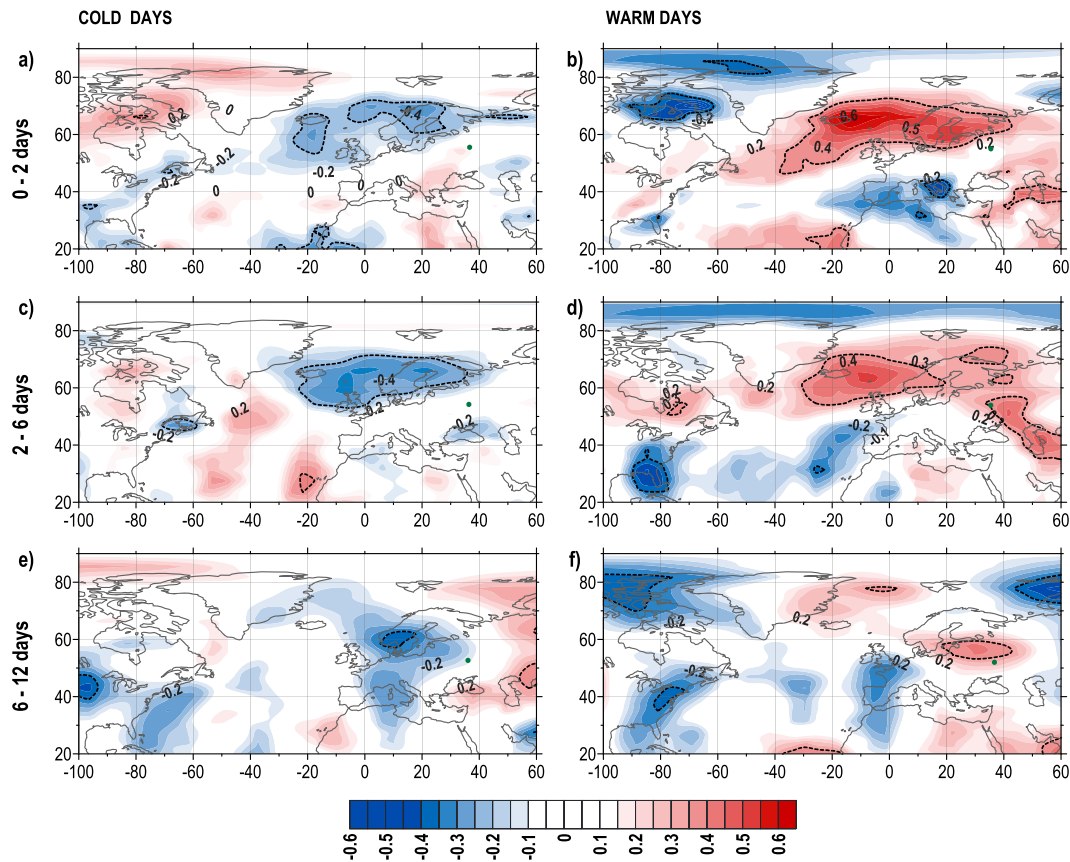
We note that trajectories obtained for the different phases of the SCAND (Figure S1) demonstrate some similarity to the NAO-related trajectories (Figure 9). Nevertheless, from statistical point of view (i.e., by their definition as the leading empirical orthogonal function modes; e.g., Barnston & Livezey, 1987) these two climate signals should be independent. Our additional analysis revealed low negative correlation between the SCAND and NAO indices (Figure S2). In-depth analysis of dependence/independence of these two teleconnections is beyond the scope of this study. Thus, we included only a brief discussion of the SCAND influence in the supporting information.

Figure 10 shows major tendencies of long-term climatic changes in the number of extremely cold and warm days in Moscow. There is rather large negative correlation ( $-0.67$ ) between the tendencies of the number of the cold and warm days. It is seen particularly that the period 1977–1997 was characterized by a positive trend in the number of warm days and by a negative trend in the number of cold days. During this period the NAO index demonstrated a positive trend (Figure 10). The opposite picture was observed from in the period 1991–2011 (Figure 10). Recently, trends have changed their signs again. Correlations between the tendencies of the NAO and the number of warm and cold days are 0.53 and  $-0.43$  respectively. Thus, these results imply that long-term wintertime changes in the number of extremely cold/warm days in Moscow are essentially driven by long-term changes in the NAO state.

### 4.3. Relationship to Large-Scale Synoptic Activity

Here we investigate links between regional atmospheric dynamics and AT extremes in Moscow. We first separate short-term (i.e., synoptic) atmospheric variability into several time scales (0–2, 2–6, and 6–12 days) by applying a Lanczos filter (e.g., Duchon, 1979) to 6-hourly  $Z_{850\text{hPa}}$  in the North Atlantic-European sector. Next, we estimate  $\sigma$  for the filtered data, thus obtaining a diagnostic for the intensity of atmospheric variability at each of the above indicated time scales. Finally, we estimate correlations between this intensity diagnostic of synoptic activity (i.e.,  $\sigma(Z_{850\text{hPa}})$ ) and time series of the number of cold and warm days in Moscow during each winter (DJF) season for 1979/1980–2016/2017 (total 38 years, Figure 11).

Correlations between time series for the number of anomalously cold days in Moscow and the intensity of the shortest (0–2 days) and synoptic (2–6 days) atmospheric processes form a pattern with significant negative correlations between Iceland and Scandinavia (Figure 11a). This implies that wintertime cold AT extremes in Moscow are associated with weakening of synoptic activity along the North Atlantic storm track. The area of negative correlation reduces when we consider links to longer-term atmospheric processes (Figures 11e). For the longest considered time scale (6–12 days) of atmospheric variability, we find a local center of large negative correlations over Scandinavia and northwestern part of European Russia



**Figure 11.** Correlation between the intensity of synoptic activity ( $\sigma(Z_{850\text{hPa}})$ ) and the number of cold days below 10th percentile (a, c, and e) and warm days exceeding 90th percentile (b, d, and f) days for December-January-February period, 1948/1949–2011/2012 (64 years). Moscow is marked by the green point. Dashed contours indicate correlations that are significant at the 5% level. Correlations shown are Pearson's correlation coefficients (i.e., parametric and linear), and significance is assessed against the associated two-tailed  $p$  values. Correlations were repeated with Spearman's coefficients (i.e., nonparametric and monotonic) and result in the same conclusions.

(Figure 11e). This implies an association between cold AT extremes in Moscow and a direct cooling triggered by a blocking-type atmospheric circulation pattern.

The correlation patterns for anomalously warm days in Moscow and the intensity of the shortest (0–2 days) atmospheric fluctuations over the North Atlantic and Europe show a major positive center of action over the northern North Atlantic and Scandinavia (Figure 11b), which reflects the local storm track. The center of significant negative correlations is seen over the Mediterranean Sea. This is almost the inverse pattern to that obtained for the anomalously cold days (Figure 11a). This pattern suggests that wintertime warm events in Moscow are associated with an intensification of the short-term synoptic activity along the North Atlantic storm track region and Scandinavia, thus with enhanced advection of relatively moist and warm air into the European region. At the same time synoptic activity over the Mediterranean Sea is weakened. Altogether this pattern is reminiscent of the SCAND teleconnection. This agrees with above revealed link between warm extremes and the SCAND (Table S1).

A similar pattern but with generally lower correlations is obtained for the longer-term (2–6 days) atmospheric variability (Figure 11d) over Scandinavia, but we do not find significant correlations over the Mediterranean Sea. The correlation pattern for the longest considered time scale (6–12 days) reveals local center of positive correlations over European Russia (Figure 11f), which is opposite to the correlation center obtained for the cold AT extremes in Moscow (Figure 11e).

These results supplement the conclusions from the trajectory analysis and associated links to the NAO in that variability of the North Atlantic and Mediterranean storm tracks play a major role in the variability

of the number of extreme days in Moscow. Changes in these storm tracks should therefore affect changes in the number of extreme events. Recent studies have shown a tendency for a poleward deflection of the storm track in the Atlantic-European region in some but not all reanalysis records (Orlanski, 1998; Tilinina et al., 2013). This tendency is also found in some model simulations corresponding to warming climate scenarios (Löptien et al., 2008; Pinto et al., 2007; Woollings & Blackburn, 2012). Such a poleward deflection of the storm track would support our results in demonstrating an increase in the number of warm events and decrease in the number of cold events.

## 5. Summary and Discussion

Here observational and reanalysis data from different data sets have been analyzed to study the major characteristics of wintertime cold and warm AT extremes in Moscow and to explore their long-term changes over recent decades. We further investigated dynamical linkages of these extremes to synoptic-scale activity in the North Atlantic-European sector and explored air mass origin implicated in their formation. A novel finding is that there is strong seasonality in the frequency distribution of daily AT anomalies in Moscow. Specifically, we found that the wintertime frequency distribution of daily AT anomalies is asymmetric and characterized by large negative skewness in contrast to the summer season, when the observed frequency distribution of daily AT anomalies in Moscow is essentially Gaussian.

We detected significant interdecadal changes in the statistical characteristics of winter AT extremes. Persistent shifts in the means for PDFs of daily AT anomalies reflect trend-like warming which has intensified since the late 1970s. This agrees with recent studies of the regional impacts of global climate change (e.g., Intergovernmental Panel on Climate Change, 2014). These changes are more pronounced during middle-to-late winter (January–March). In particular, our analysis revealed a significant long-term decrease in intraseasonal AT variability, which is most pronounced during late January to early February. This result is broadly consistent with findings of Screen (2014) who studied Arctic amplification and revealed that it results in a decrease of the intraseasonal temperature variance in the middle to high latitudes. We detect changes in the shape of PDFs, reflected by their changing skewness,  $\sigma$ , and absolute range. These changes are different in different winter months. Specifically, in December and March the probability of the cold events decreases, whereas in January the probability of cold events does not change significantly. Concurrently, the probability of warm events relative to the early climate period increases during all months. It should be stressed that in January, the absolute range covered by PDFs increased over recent decades by more than 6 °C, thus indicating an increased probability of more intense extremes, that is, higher absolute temperature values, of both cold and warm types.

This analysis additionally reveals long-term trend-like changes reflecting a general tendency toward a decrease in the number of extremely cold days and a corresponding increase in the number of extremely warm days in Moscow during winter. This is broadly consistent with the results of Andrade et al. (2012) who demonstrated evidence for a general increase in the occurrence of warm days along with a decrease in the occurrence of cold nights throughout Europe.

An analysis of linkages to regional-scale atmospheric dynamics reveals that cold wintertime AT extremes in Moscow are associated with weakening of the North Atlantic storm track activity at the shorter (few days) synoptic time scale. Warm extreme AT events are linked to intensification of the North Atlantic storm track and weakening of Mediterranean synoptic activity. The impact of atmospheric variability at longer time scales (6–12 days) upon the extreme events is more local, and in general, represented by blocking-type atmospheric patterns. We note that recent studies have demonstrated that wintertime blockings are generally associated with colder than average conditions over large regions of Europe (e.g., Sousa et al., 2018). These results are corroborated by a Lagrangian analysis of back trajectories associated with wintertime extreme events in Moscow, which reveals that cold extreme events are mostly formed by the air masses with their origin in Siberia and the northeastern North Atlantic-Arctic sector between Scandinavia and Greenland. Meanwhile, warm extreme events are triggered by advection of warm air from the western North Atlantic and Mediterranean regions. To the best of our knowledge, a quantitative assessment of this kind into the relative roles of different air mass origins in the formation of winter temperature extremes in Moscow is provided for the first time in the present study. Analysis of linkages to regional atmospheric teleconnections has revealed that interannual changes in the number of cold events

are governed mostly by the NAO–. Interannual changes in the number of warm events are driven by both the NAO+ and the SCAND– teleconnections.

To summarize results related to regional atmospheric dynamics and highlight major physical mechanisms responsible, here we briefly describe the sequence of events resulting in AT extremes in Moscow. The persistence of an increased meridional pressure gradient over the North Atlantic, corresponding to the positive phase of the NAO, results in intensification of the North Atlantic storm track reflected in the enhanced synoptic activity in the respective region. This results in increased advection of warm and wet air into the European region resulting in positive AT anomalies in Moscow. In addition to this, the presence of a large-scale cyclonic anomaly over Scandinavia and the BKS basin, corresponding to the negative phase of the SCAND teleconnection, favors warm air advection from the North Atlantic and Mediterranean Sea regions, which also results in above average AT in Moscow. During the negative phase of the NAO the reduced meridional pressure gradient over the North Atlantic results in weakening of the North Atlantic storm track and a suppression of synoptic activity which generally favors formation of the blocking-type atmospheric anomalies. This eventually results in cold extremes in Moscow.

While we explored in detail the dynamical linkages of AT extremes formation to regional atmospheric variability, there are other factors that are potentially relevant. This comment particularly refers to large decadal-scale changes in the characteristics of AT extremes revealed in the present analysis. However, to get a robust assessment of such changes and their possible driving mechanisms, high-resolution data covering a longer time period are needed. Experiments using hierarchies of climate models should prove very useful indeed. Although we leave this factor analysis for further study, it is worth mentioning that such phenomena as the Atlantic Multidecadal Oscillation (e.g., Enfield et al., 2001; Hao et al., 2016) might play a role (through influence on the North Atlantic storm track) in winter AT extremes in Moscow and over European Russia. Results of a recent study (Shukurov & Semenov, 2018) suggest an impact of reduced sea ice concentration in the Barents Sea on the wintertime AT anomalies in Moscow, which is broadly consistent with other recent work (Screen, 2014; Tang et al., 2013). Screen (2017b) showed that sea ice reduction specifically in that location could be associated with a weakening of the stratospheric polar vortex and a subsequent tropospheric response that resembles the NAO. This connection appears to be consistent with our results also.

Although the so-called Ural Blocking is associated with both the NAO and sea ice loss in the BKS basin (Luo, Xiao, Diao, et al., 2016; Luo, Xiao, Yao, et al., 2016), and thus is not independent from these phenomena, its possible impact on winter temperature extremes in Moscow will be explored in a separate study. Hence, a possible effect of these remote climate signals on the winter AT extremes in Moscow is of significant interest and deserves further investigation. Thus, we believe that additional diagnostic studies of the observational record will have merit in addition to advanced model experiments, which will allow for a more accurate assessment of driving mechanisms and their relative roles in wintertime temperature extremes in Moscow.

#### Acknowledgments

All authors contributed equally to this work, and the original idea came from Y. Z. and I. Z. Discussions with Sergey Gulev have been very valuable and are greatly appreciated. J. H. P. S. is extremely grateful to Michael Sprenger of ETH Zurich for advice on Lagrangian analysis and to Michael Sprenger and Heini Werni for making their code freely available for use. We thank the anonymous reviewers for their comments and suggestions that have greatly improved the manuscript. Talks with Vladimir Semenov are also greatly appreciated. We are grateful to the All Russian Research Institute of Hydrometeorological Information-World Data Center (Federal Service of Russia for Hydrometeorology and Monitoring Environment), ECMWF, and NOAA for making their data publicly available at the following addresses: <http://meteo.ru/data/162-temperature-precipitation>, <http://apps.ecmwf.int/datasets/data/interim-full-daily>, and <http://www.cpc.ncep.noaa.gov/data/teledoc/telecontents.shtml>, respectively. This research was supported by the Russian Science Foundation grant 18-47-06202 (J.H.P.S., Y.Z.) and by the project 14.B25.31.0026 of the Ministry of Education and Science of the Russian Federation (I.Z.).

#### References

- Alexander, L. V., Zhang, X., Peterson, T. C., Caesar, J., Gleason, B., Tank, A. K., et al. (2006). Global observed changes in daily climate extremes of temperature and precipitation. *Journal of Geophysical Research*, *111*, D05109. <https://doi.org/10.1029/2005JD006290>
- Andrade, C., Leite, S. M., & Santos, J. A. (2012). Temperature extremes in Europe: Overview of their driving atmospheric patterns. *Natural Hazards and Earth System Sciences*, *12*(5), 1671–1691. <https://doi.org/10.5194/nhess-12-1671-2012>
- Ballester, J., Douville, H., & Chauvin, F. (2009). Present-day climatology and projected changes of warm and cold days in the CNRM-CM3 global climate model. *Climate Dynamics*, *32*(1), 35–54. <https://doi.org/10.1007/s00382-008-0371-0>
- Barnston, A. G., & Livezey, R. E. (1987). Classification, seasonality and persistence of low-frequency atmospheric circulation patterns. *Monthly Weather Review*, *115*(6), 1083–1126. [https://doi.org/10.1175/1520-0493\(1987\)115<1083:CSAPOL>2.0.CO;2](https://doi.org/10.1175/1520-0493(1987)115<1083:CSAPOL>2.0.CO;2)
- Barriopedro, D., Fischer, E. M., Luterbacher, J., Trigo, R. M., & García-Herrera, R. (2011). The hot summer of 2010: Redrawing the temperature record map of Europe. *Science*, *332*(6026), 220–224. <https://doi.org/10.1126/science.1201224>
- Bendat, J. S., & Piersol, A. G. (1966). *Measurement and analysis of random data* (p. 390). New York: John Wiley.
- Beniston, M. (2004). The 2003 heat wave in Europe: A shape of things to come? An analysis based on Swiss climatological data and model simulations. *Geophysical Research Letters*, *31*, L02202. <https://doi.org/10.1029/2003GL018857>
- Bindoff, N. L., Stott, P. A., AchutaRao, K. M., Allen, M. R., Gillett, N., Gutzler, D., et al. (2013). Detection and attribution of climate change: From global to regional. In T. F. Stocker et al. (Eds.), *Climate change 2013: The physical science basis. Contribution of Working Group I to the Fifth Assessment Report of the Intergovernmental Panel on Climate Change* (pp. 867–952). Cambridge: Cambridge University Press. <https://doi.org/10.1017/CBO9781107415324.022>
- Borodina, A., Fischer, E. M., & Knutti, R. (2017). Potential to constrain projections of hot temperature extremes. *Journal of Climate*, *30*(24), 9949–9964. <https://doi.org/10.1175/JCLI-D-16-0848.1>

- Cattiaux, J., Vautard, R., Cassou, C., Yiou, P., Masson-Delmotte, V., & Codron, F. (2010). Winter 2010 in Europe: A cold extreme in a warming climate. *Geophysical Research Letters*, *37*, L20704. <https://doi.org/10.1029/2010GL044613>
- Chen, X., & Luo, D. (2017). Arctic sea ice decline and continental cold anomalies: Upstream and downstream effects of Greenland blocking. *Geophysical Research Letters*, *44*, 3411–3419. <https://doi.org/10.1002/2016GL072387>
- Christensen, J. H., Hewitson, B., Busuioc, A., Chen, A., Gao, X., Held, R., et al. (2007). Regional climate projections. In *Climate change, 2007: The physical science basis. Contribution of Working Group I to the Fourth Assessment Report of the Intergovernmental Panel on Climate Change* (Chapter 11, pp. 847–940). Cambridge University Press.
- Cohen, J., Screen, J. A., Furtado, J. C., Barlow, M., Whittleston, D., Coumou, D., et al. (2014). Recent Arctic amplification and extreme mid-latitude weather. *Nature Geoscience*, *7*(9), 627–637. <https://doi.org/10.1038/ngeo2234>
- Cohen, J. L., Furtado, J. C., Barlow, M. A., Alexeev, V. A., & Cherry, J. E. (2012). Arctic warming, increasing snow cover and widespread boreal winter cooling. *Environmental Research Letters*, *7*(1), 014007. <https://doi.org/10.1088/1748-9326/7/1/014007>
- Coles, S., Bawa, J., Trenner, L., & Dorazio, P. (2001). *An introduction to statistical modeling of extreme values* (Vol. 208). London: Springer. <https://doi.org/10.1007/978-1-4471-3675-0>
- Coumou, D., & Rahmstorf, S. (2012). A decade of weather extremes. *Nature Climate Change*, *2*(7), 491–496. <https://doi.org/10.1038/nclimate1452>
- de Vries, H., Haarsma, R. J., & Hazeleger, W. (2012). Western European cold spells in current and future climate. *Geophysical Research Letters*, *39*, L04706. <https://doi.org/10.1029/2011GL050665>
- Dee, D. P., Uppala, S. M., Simmons, A. J., Berrisford, P., Poli, P., Kobayashi, S., et al. (2011). The ERA-interim reanalysis: Configuration and performance of the data assimilation system. *Quarterly Journal of the Royal Meteorological Society*, *137*(656), 553–597. <https://doi.org/10.1002/qj.828>
- Diao, Y., Xie, S. P., & Luo, D. (2015). Asymmetry of winter European surface air temperature extremes and the North Atlantic Oscillation. *Journal of Climate*, *28*(2), 517–530. <https://doi.org/10.1175/JCLI-D-13-00642.1>
- Donat, M. G., Lowry, A. L., Alexander, L. V., O’Gorman, P. A., & Maher, N. (2016). More extreme precipitation in the world’s dry and wet regions. *Nature Climate Change*, *6*(5), 508–513. <https://doi.org/10.1038/nclimate2941>
- Dosio, A., & Fischer, E. M. (2018). Will half a degree make a difference? Robust projections of indices of mean and extreme climate in Europe under 1.5 °C, 2 °C, and 3 °C global warming. *Geophysical Research Letters*, *45*, 935–944. <https://doi.org/10.1002/2017GL076222>
- Duchon, C. E. (1979). Lanczos filtering in one and two dimensions. *Journal of Applied Meteorology*, *18*(8), 1016–1022. [https://doi.org/10.1175/1520-0450\(1979\)018<1016:LFOAT>2.0.CO;2](https://doi.org/10.1175/1520-0450(1979)018<1016:LFOAT>2.0.CO;2)
- Dwyer, J. G., & O’Gorman, P. A. (2017). Changing duration and spatial extent of midlatitude precipitation extremes across different climates. *Geophysical Research Letters*, *44*, 5863–5871. <https://doi.org/10.1002/2017GL072855>
- Enfield, D. B., Mestas-Núñez, A. M., & Trimble, P. J. (2001). The Atlantic multidecadal oscillation and its relation to rainfall and river flows in the continental US. *Geophysical Research Letters*, *28*, 2077–2080. <https://doi.org/10.1029/2000GL012745>
- Folland, C. K., Miller, C., Bader, D., Crowe, M., Jones, P., Plummer, N., et al. (1999). Workshop on indices and indicators for climate extremes, Asheville, NC, USA, 3–6 June 1997 Breakout Group C: Temperature indices for climate extremes. *Climatic Change*, *42*(1), 31–43. <https://doi.org/10.1023/A:1005447712757>
- Francis, J. A., & Vavrus, S. J. (2012). Evidence linking Arctic amplification to extreme weather in mid-latitudes. *Geophysical Research Letters*, *39*, L06801. <https://doi.org/10.1029/2012GL051000>
- Fuchs, J., Cermak, J., Andersen, H., Hollmann, R., & Schwarz, K. (2017). On the influence of air mass origin on low-cloud properties in the Southeast Atlantic. *Journal of Geophysical Research: Atmospheres*, *122*, 11,076–11,091. <https://doi.org/10.1002/2017JD027184>
- Gulev, S. K., & Belyaev, K. (2012). Probability distribution characteristics for surface air–sea turbulent heat fluxes over the global ocean. *Journal of Climate*, *25*(1), 184–206. <https://doi.org/10.1175/2011JCLI4211.1>
- Hannachi, A., Jolliffe, I. T., & Stephenson, D. B. (2007). Empirical orthogonal functions and related techniques in atmospheric science: A review. *International Journal of Climatology: A Journal of the Royal Meteorological Society*, *27*(9), 1119–1152. <https://doi.org/10.1002/joc.1499>
- Hao, X., He, S., & Wang, H. (2016). Asymmetry in the response of central Eurasian winter temperature to AMO. *Climate Dynamics*, *47*(7–8), 2139–2154. <https://doi.org/10.1007/s00382-015-2955-9>
- Holton, J. R., & Hakim, G. J. (2013). *An introduction to dynamic meteorology* (532 pp.). New York: Academic Press.
- Hurrell, J. W. (1995). Decadal trends in the North Atlantic Oscillation: Regional temperatures and precipitation. *Science*, *269*(5224), 676–679. <https://doi.org/10.1126/science.269.5224.676>
- Intergovernmental Panel on Climate Change (2012). In C. B. Field, V. Barros, T. F. Stocker, & Q. Dahe (Eds.), *Managing the risks of extreme events and disasters to advance climate change adaptation: Special report of the intergovernmental panel on climate change*. Cambridge: Cambridge University Press.
- Intergovernmental Panel on Climate Change (2014). Summary for Policymakers. In *Climate Change 2013 – The Physical Science Basis: Working Group I Contribution to the Fifth Assessment Report of the Intergovernmental Panel on Climate Change* (pp. 1–30). Cambridge: Cambridge University Press. <https://doi.org/10.1017/CBO9781107415324.004>
- Klein Tank, A. M. G., Zwiers, F. W., & Zhang, X. (2009). Guidelines on analysis of extremes in a changing climate in support of informed decisions for adaptation. *World Meteorological Organization*. (WCDMP-72, WMO-TD/No. 1500), 56.
- Lloyd, S. (1982). Least squares quantization in PCM. *IEEE Transactions on Information Theory*, *28*(2), 129–137. <https://doi.org/10.1109/TIT.1982.1056489>
- Löptien, U., Zolina, O., Gulev, S., Latif, M., & Soloviev, V. (2008). Cyclone life cycle characteristics over the Northern Hemisphere in coupled GCMs. *Climate Dynamics*, *31*(5), 507–532. <https://doi.org/10.1007/s00382-007-0355-5>
- Luo, D. (2005). Why is the North Atlantic block more frequent and long-lived during the negative NAO phase? *Geophysical Research Letters*, *32*, L20804. <https://doi.org/10.1029/2005GL022927>
- Luo, D., Xiao, Y., Diao, Y., Dai, A., Franzke, C. L., & Simmonds, I. (2016). Impact of Ural blocking on winter warm Arctic–cold Eurasian anomalies. Part II: The link to the North Atlantic Oscillation. *Journal of Climate*, *29*(11), 3949–3971. <https://doi.org/10.1175/JCLI-D-15-0612.1>
- Luo, D., Xiao, Y., Yao, Y., Dai, A., Simmonds, I., & Franzke, C. L. (2016). Impact of Ural blocking on winter warm Arctic–cold Eurasian anomalies. Part I: Blocking-induced amplification. *Journal of Climate*, *29*(11), 3925–3947. <https://doi.org/10.1175/JCLI-D-15-0611.1>
- Moore, G. W. K., Renfrew, I. A., & Pickart, R. S. (2013). Multidecadal mobility of the North Atlantic oscillation. *Journal of Climate*, *26*(8), 2453–2466. <https://doi.org/10.1175/JCLI-D-12-00023.1>



- Orlanski, I. (1998). Poleward deflection of storm tracks. *Journal of the Atmospheric Sciences*, 55(16), 2577–2602. [https://doi.org/10.1175/1520-0469\(1998\)055<2577:PDOST>2.0.CO;2](https://doi.org/10.1175/1520-0469(1998)055<2577:PDOST>2.0.CO;2)
- Overland, J. E., Dethloff, K., Francis, J. A., Hall, R. J., Hanna, E., Kim, S. J., et al. (2016). Nonlinear response of mid-latitude weather to the changing Arctic. *Nature Climate Change*, 6(11), 992–999. <https://doi.org/10.1038/nclimate3121>
- Overland, J. E., Wood, K. R., & Wang, M. (2011). Warm Arctic-cold continents: Climate impacts of the newly open Arctic Sea. *Polar Research*, 30(1), 15787. <https://doi.org/10.3402/polar.v30i0.15787>
- Papritz, L., & Spengler, T. (2017). A Lagrangian climatology of wintertime cold air outbreaks in the Irminger and Nordic Seas and their role in shaping air–sea heat fluxes. *Journal of Climate*, 30(8), 2717–2737. <https://doi.org/10.1175/JCLI-D-16-0605.1>
- Pedregosa, F., Varoquaux, G., Gramfort, A., Michel, V., Thirion, B., Grisel, O., et al. (2011). Scikit-learn: Machine learning in Python. *Journal of Machine Learning Research*, 12(Oct), 2825–2830.
- Pfahl, S., O’Gorman, P. A., & Fischer, E. M. (2017). Understanding the regional pattern of projected future changes in extreme precipitation. *Nature Climate Change*, 7(6), 423–427. <https://doi.org/10.1038/nclimate3287>
- Pinto, J. G., Ulbrich, U., Leckebusch, G. C., Spanghel, T., Meyers, M., & Zacharias, S. (2007). Changes in storm track and cyclone activity in three SRES ensemble experiments with the ECHAM5/MPI-OM1 GCM. *Climate Dynamics*, 29(2–3), 195–210. <https://doi.org/10.1007/s00382-007-0230-4>
- Razuvaev, V. N., Apasova, E. G., Martuganov, R. A., Vose, R. S., & Steurer, P. M. (1993). Daily temperature and precipitation data for 223 USSR stations (No. ORNL/CDIAC-56; NDP-040). Oak Ridge National Lab., TN (United States). <https://doi.org/10.2172/10154823>
- Schär, C., Vidale, P. L., Lüthi, D., Frei, C., Häberli, C., Liniger, M. A., & Appenzeller, C. (2004). The role of increasing temperature variability in European summer heatwaves. *Nature*, 427(6972), 332–336. <https://doi.org/10.1038/nature02300>
- Schemm, S., Ciasto, L. M., Li, C., & Kvamstø, N. G. (2016). Influence of tropical Pacific Sea surface temperature on the genesis of Gulf Stream cyclones. *Journal of the Atmospheric Sciences*, 73(10), 4203–4214. <https://doi.org/10.1175/JAS-D-16-0072.1>
- Schemm, S., & Schneider, T. (2018). Eddy lifetime, number, and diffusivity and the suppression of eddy kinetic energy in midwinter. *Journal of Climate*, 31(14), 5649–5665. <https://doi.org/10.1175/JCLI-D-17-0644.1>
- Screen, J. A. (2014). Arctic amplification decreases temperature variance in northern mid- to high-latitudes. *Nature Climate Change*, 4(7), 577–582. <https://doi.org/10.1038/nclimate2268>
- Screen, J. A. (2017a). The missing northern European winter cooling response to Arctic sea ice loss. *Nature Communications*, 8, 14603. <https://doi.org/10.1038/ncomms14603>
- Screen, J. A. (2017b). Simulated atmospheric response to regional and pan-Arctic sea ice loss. *Journal of Climate*, 30(11), 3945–3962. <https://doi.org/10.1175/JCLI-D-16-0197.1>
- Screen, J. A., & Simmonds, I. (2014). Amplified mid-latitude planetary waves favour particular regional weather extremes. *Nature Climate Change*, 4(8), 704–709. <https://doi.org/10.1038/nclimate2271>
- Serreze, M. C., & Francis, J. A. (2006). The Arctic amplification debate. *Climatic Change*, 76(3–4), 241–264. <https://doi.org/10.1007/s10584-005-9017-y>
- Shepherd, T. G. (2016). Effects of a warming Arctic. *Science*, 353(6303), 989–990. <https://doi.org/10.1126/science.aag2349>
- Shukurov, K. A., & Semenov, V. A. (2018). Characteristics of winter surface air temperature anomalies in Moscow in 1970–2016 under conditions of reduced sea ice area in the Barents Sea. *Izvestiya, Atmospheric and Oceanic Physics*, 54(1), 10–24. <https://doi.org/10.1134/S0001433818010115>
- Sillmann, J., Croci-Maspoli, M., Kallache, M., & Katz, R. W. (2011). Extreme cold winter temperatures in Europe under the influence of North Atlantic atmospheric blocking. *Journal of Climate*, 24(22), 5899–5913. <https://doi.org/10.1175/2011JCLI4075.1>
- Sousa, P. M., Trigo, R. M., Barriopedro, D., Soares, P. M., & Santos, J. A. (2018). European temperature responses to blocking and ridge regional patterns. *Climate Dynamics*, 50(1–2), 457–477. <https://doi.org/10.1007/s00382-017-3620-2>
- Sprenger, M., & Wernli, H. (2015). The LAGRANTO Lagrangian analysis tool—version 2.0. *Geoscientific Model Development*, 8(8), 2569–2586. <https://doi.org/10.5194/gmd-8-2569-2015>
- Sura, P. (2014). Climate: Extreme events. In *Encyclopedia of natural resources: Air* (pp. 986–989). New York: Taylor and Francis. <https://doi.org/10.1081/E-ENRA-120047635>
- Tang, Q., Zhang, X., Yang, X., & Francis, J. A. (2013). Cold winter extremes in northern continents linked to Arctic sea ice loss. *Environmental Research Letters*, 8(1), 014036. <https://doi.org/10.1088/1748-9326/8/1/014036>
- Tibaldi, C., Hayhoe, K., Arblaster, J. M., & Meehl, G. A. (2006). Going to the extremes. *Climatic Change*, 79(3–4), 185–211. <https://doi.org/10.1007/s10584-006-9051-4>
- Tilina, N., Gulev, S. K., Rudeva, I., & Koltermann, P. (2013). Comparing cyclone life cycle characteristics and their interannual variability in different reanalyses. *Journal of Climate*, 26(17), 6419–6438. <https://doi.org/10.1175/JCLI-D-12-00777.1>
- Tyrlis, E., & Hoskins, B. J. (2008). Aspects of a Northern Hemisphere atmospheric blocking climatology. *Journal of the Atmospheric Sciences*, 65(5), 1638–1652. <https://doi.org/10.1175/2007JAS2337.1>
- United Nations, Department of Economic and Social Affairs, Population Division (2015). World urbanization prospects: The 2014 revision, (ST/ESA/SER.A/366).
- Wang, C., Liu, H., & Lee, S. K. (2010). The record-breaking cold temperatures during the winter of 2009/2010 in the Northern Hemisphere. *Atmospheric Science Letters*, 11(3), 161–168. <https://doi.org/10.1002/asl.278>
- Woollings, T., Barriopedro, D., Methven, J., Son, S. W., Martius, O., Harvey, B., et al. (2018). Blocking and its response to climate change. *Current Climate Change Reports*, 4(3), 287–300. <https://doi.org/10.1007/s40641-018-0108-z>
- Woollings, T., & Blackburn, M. (2012). The North Atlantic jet stream under climate change and its relation to the NAO and EA patterns. *Journal of Climate*, 25(3), 886–902. <https://doi.org/10.1175/JCLI-D-11-00087.1>
- World Meteorological Organisation (2015). Technical regulations, Vol. 1: General meteorological standards and recommended practices. WMO. Geneva.
- Zhang, X., Hegerl, G., Zwiers, F. W., & Kenyon, J. (2005). Avoiding inhomogeneity in percentile-based indices of temperature extremes. *Journal of Climate*, 18(11), 1641–1651. <https://doi.org/10.1175/JCLI3366.1>
- Zhong, L., Hua, L., & Luo, D. (2018). Local and external moisture sources for the Arctic warming over the Barents–Kara seas. *Journal of Climate*, 31(5), 1963–1982. <https://doi.org/10.1175/JCLI-D-17-0203.1>
- Zhou, X., & Khairoutdinov, M. F. (2017). Changes in temperature and precipitation extremes in superparameterized CAM in response to warmer SSTs. *Journal of Climate*, 30(24), 9827–9845. <https://doi.org/10.1175/JCLI-D-17-0214.1>
- Zveryaev, I. I. (2006). Seasonally varying modes in long-term variability of European precipitation during the 20th century. *Journal of Geophysical Research*, 111, D21116. <https://doi.org/10.1029/2005JD006821>

- Zveryaev, I. I. (2007). Climatology and long-term variability of the annual cycle of air temperature over Europe. *Russian Meteorology and Hydrology*, 32(7), 426–430. <https://doi.org/10.3103/S1068373907070023>
- Zveryaev, I. I., & Gulev, S. K. (2009). Seasonality in secular changes and interannual variability of European air temperature during the twentieth century. *Journal of Geophysical Research*, 114, D02110. <https://doi.org/10.1029/2008JD010624>
- Zwillinger, D. (2002). *CRC standard mathematical tables and formulae*. Boca Raton, FL: Chapman and Hall/CRC. <https://doi.org/10.1201/9781420035346>
- Zyulyaeva, Y. A., Zveryaev, I. I., & Koltermann, K. P. (2016). Observations-based analysis of the summer temperature extremes in Moscow. *International Journal of Climatology*, 36(2), 607–617. <https://doi.org/10.1002/joc.4370>